High Performance Polymers

Changes induced in the properties of dielectric silicone elastomers by the incorporation of transition metal complexes

Journal:	*High Performance Polymers*
Manuscript ID	HPP-15-0326.R1
Manuscript Type:	Original Manuscript
Keywords:	silicone elastomers, polymer composites, dielectric properties, tensile testing, metal complexes

Abstract:	Three new, cheap and easily obtained complexes of triethanolamine with Cu(II), Ni(II) and Co(II) were incorporated in a high molecular weight polydimethylsiloxane-α,ω-diol (Mn= 440000 g·mol-1) together with silica nanoparticles. While silica has a well-known mechanical reinforcing role, adding the metal complexes with high dielectric permittivity aims to increase values for this characteristic of the prepared silicone matrix samples, in order to be useful for electromechanical applications. A simple procedure was employed for the fillers' incorporation by mechanical mixing, in bulk without a solvent. The composites were processed as films and stabilized by curing initiated by 2,4-dichlorobenzoyl peroxide at high temperature (180 oC) and pressure. The crosslinking yield was estimated on the basis of swelling in chloroform, while the crosslinking density, ρc (mol·cm-3), was calculated from differential scanning calorimetry traces. The filler's effect on mechanical and dielectric properties was assessed by appropriate measurements (tensile testing, dielectric spectroscopy). Changes in dielectric behavior as a result of the repeated deformation by stretching were also highlighted. Electromechanical sensitivity and ultimate tensile toughness values were estimated on the basis of these results as primary indications on suitability of these materials in transducers. The dielectric strength of the composite films was also evaluated by electrical breakdown field (EBD) measurements.

Changes induced in the properties of dielectric silicone elastomers by the incorporation of transition metal complexes

Abstract

Three new, cheap and easily obtained complexes of triethanolamine with Cu(II), Ni(II) and Co(II) were incorporated in a high molecular weight polydimethylsiloxane-α,ω-diol (Mn= 440000 g·mol^{-1}) together with silica nanoparticles. While silica has a well-known mechanical reinforcing role, adding the metal complexes with high dielectric permittivity aims to increase values for this characteristic of the prepared silicone matrix samples, in order to be useful for electromechanical applications. A simple procedure was employed for the fillers' incorporation by mechanical mixing, in bulk without a solvent. The composites were processed as films and stabilized by curing initiated by 2,4-dichlorobenzoyl peroxide at high temperature (180 ^{o}C) and pressure. The crosslinking yield was estimated on the basis of swelling in chloroform, while the crosslinking density, ρ_c (mol·cm^{-3}), was calculated from differential scanning calorimetry traces. The filler's effect on mechanical and dielectric properties was assessed by appropriate measurements (tensile testing, dielectric spectroscopy). Changes in dielectric behavior as a result of the repeated deformation by stretching were also highlighted. Electromechanical sensitivity and ultimate tensile toughness values were estimated on the basis of these results as primary indications on suitability of these materials in transducers. The dielectric strength of the composite films was also evaluated by electrical breakdown field (EBD) measurements.

***Keywords*:** silicone elastomers; polymer composites; dielectric properties; tensile testing; metal complexes

1. Introduction

Dielectric elastomer actuators (DEA) are electric-field-electroactive polymers (EAP), a subgroup of the family of electroactive polymers[1] and have the capability to expand the surface more than 100% under an external electric field.[2] This large strain makes DEA suitable for applications such as artificial muscles, for haptic devices,[3] valves[4] and pumps as well as the control of optical components,[5] soft robots, adaptive optics, Braille displays and electric generators.[6–9] For such applications, it is necessary to use a material which possesses large displacement with high precision and speed when actuated, together with durability and reliability, low stiffness (low values for Young's modulus), high breakdown strength, and high permittivity.[10] Silicones have highly desired elastic behaviour, their representative polydimethylsiloxane-α,ω-diol (PDMS) being known for its non-Newtonian rheological/flow properties.[11] Silicone elastomers show also some characteristics that make them the preferred material for use in DEA: a high electric breakdown field strength of more than 50 kV/mm, a low uptake of water due to their hydrophobic character, the ability to function in a broad temperature range, from -60 °C to upwards of 200 °C, and the capability to be processed into thin flexible films. A disadvantage of silicone elastomers is their low relative permittivity (ε' = 2.8 – 3), which limits the actuation strain according to established correlation.[12–14] Researchers have tried to obtain silicones with enhanced values of permittivity, and this, in turn, allows increased values for the actuation strain and the Maxwell pressure of silicone elastomer. One of the ways of enhancing the dielectric properties of the silicones consists of their mixing in various adequate fillers.[15–19] There are several types of fillers used to improve the permittivity of the dielectric elastomers: ceramic particles with a high dielectric constant;[18,20–23] conductive particles (carbon nanotubes, carbon black, copper–phthalocyanine/polyaniline)[24] and short fibers;[22] highly polarizable conjugated

polymers such as undoped poly(3-hexyltiophene), polyaniline, polythiophene - incorporated by bulk blending or as nanoparticles.[12,18,22,25–28] Pure metal particles were used as fillers for improving the dielectric properties of elastomers, such as copper nanoparticles incorporated in silica particles[29] and aluminum nanoparticles in an acrylate elastomer[30]. Due to the known incompatibility of the silicones with almost every other component, especially if this is a polar one, the resulting materials often have worsened mechanical properties compared to the pure matrix and this could be the cause for reduced values of strain of the elastomer film in the electric field.

In this work, we used as fillers for silicone, complexes of Cu(II), Ni(II) and Co(II) with triethanolamine, whose preparation and structural characterization were reported in previous papers.[31,32] It is expected that the polarity of the compounds due to the metal coordinated units to induce an increase in dielectric permittivity of the resulted composites, while the ethylene bridges belonging to the ligand can ensure compatibility with hydrophobic silicone matrix, thus preserving its good mechanical properties. The structure of the metal complexes used in this work leads to avoiding the use of compatibilizing agents and surface treatments for the particles of filler. Also, the preparation process aims to preserve the low value of Young modulus and dielectric behaviour of pure siloxanes, as such characteristics are required for use as dielectric elastomers. Therefore the preparation of the samples tries to balance the goal of improving the dielectric permitivitty of the prepared dielectric elastomer with the required flexibility (low Young modulus) and dielectric nature of the siloxanes in dielectric actuation and energy harvesting. In this aim, complexes finely powdered by manual grinding were incorporated by mechanical mixing within a silicone consisting of a polydimethylsiloxane-α,ω-diol of high molecular mass (M_n = 440000 g·mol^{-1}). The mixture was molded in a thin rectangular shape and

cured by a radicalic mechanism under high pressure. The resulting free standing films were characterized for thermal, moisture behavior, mechanical and dielectric points of view.

2. Experimental

2.1. Materials

The copper complex $C_{12}H_{29.85}Cu_{2.07}Cl_4N_2O_6$, CuC, (M = 571.78), consisting of ionic dinuclear $[Cu_2(H_3L)_2Cl_2]Cl_2$ co-crystallized with molecular tetranuclear $[Cu_4(HL)_2Cl_4]$ species in a 1:0.036 ratio, and the nickel complex $C_{12}H_{30}Ni_2Cl_4N_2O_6$, NiC, (M = 557.60) all possessing an atrane structure were prepared and characterized according to a previously described procedure[31] by treating proper metal chloride with triethanolamine. The cobalt complex $C_6H_{14}CoClNO_3$, CoC, (M=242.56) cobaltrane resulted when cobalt chloride was treated with 1-(3-aminopropyl)silatrane in presence of 2,4-dihydroxybenzaldehyde.[32]

2,4-Dichlorobenzoyl peroxide (DCBP), as paste 50% in silicone oil, having a critical temperature 60 -70 ^oC and set-cure temperature in the range 115 – 150 ^oC.

Polydimethylsiloxane-α,ω-diol (PDMS) matrix was synthesized by bulk polymerization of octamethylcyclotetrasiloxane with H_2SO_4 as the catalyst, at room temperature and atmospheric humidity, according to an already described procedure.[33,34] The average molecular mass for the prepared polymer as estimated by gel permeation chromatography with $CHCl_3$ as the eluent was M_n = 440000 g·mol^{-1}, with polydispersity index ($I=M_w/M_n$) of 1.4.

Fumed silica, Aerosil 200 (Degussa), 100% purity, specific surface 380 m^2/g, particle diameter 0.003-0.015 μm, was used after hydrophobization by treatment with octamethylcyclotetrasiloxane for 3 h at 180 ºC.

2.2. Equipments

SEM images of film surfaces fractured in liquid nitrogen were taken with Electron Microscope (ESEM) type Quanta 200 operating until 30 kV with secondary and backscattering electrons in low or high vacuum mode. An Energy Dispersive X-Ray system (EDX) available on SEM equipment was also used for qualitative analysis and elemental mapping.

The measurements for *Dynamic Vapour Sorption (DVS) and sorption hysteresis* were performed with an IGAsorp Dynamic Vapour Sorption apparatus with the following characteristics: resolution of 0.1 μg for 100 mg and sample containers made out of stainless steel micron size mesh. Before sorption measurements, the samples were dried at 25 ºC with dry nitrogen (250 mL/min) until the weight of the sample was in equilibrium at a relative humidity (RH) less than 1%. The measurements were performed with a program involving step increases of 10% for the relative humidity of the controlled flow of nitrogen and recording the mass change for each step.

DSC measurements were conducted with a DSC 200 F3 Maia (Netzsch, Germany). About 10 mg of sample was heated in pressed and punched aluminium crucibles at a heating rate of 10 ºC·min^{-1}. Nitrogen was used as inert atmosphere at a flow rate of 100 mL min^{-1}.

Swelling experiments were conducted using crosslinked samples previously extracted in chloroform, dried in vacuum at 50 ºC and maintained over P_2O_5 for one week in order to determine the swelling capacity in two solvents: water and chloroform. The extent of swelling of the crosslinked polymers was determined gravimetrically. After a soaking period of 48 h in solvent, each sample was removed from the respective vial, tapped with filter paper to remove the excess surface solvent, and weighed. The gels were dried at 50 ºC in vacuum to constant weight and kept over P_2O_5.

Stress–strain measurements were performed on a TIRA test 2161 apparatus, Maschinenbau GmbH Ravenstein, Germany on dumbbell-shaped cut samples with dimensions of 50x8.5x4 mm. Measurements were run at an extension rate of 20 mm/min at room temperature. All samples were measured three times and the averages of the obtained values were taken into consideration. *Dielectric spectroscopy* was performed using the Novocontrol "Concept 40" broadband dielectric spectrometer (Hundsangen, Germany). The samples were mounted between gold platens and positioned in the Novocontrol Quatro Cryosystem. The dielectric experiment was carried out at 25 ºC sweeping the frequency. Six intervals (log scale) of frequency, i.e. 1–100000 Hz, were scanned, with the dielectric constant (ε') and loss (ε") were recorded in the frequency domain (1 Hz–1 MHz). Each metal complex used as filler for the elastomer was ground to a fine powder in an agate mortar, and the powder was pressed with a 10-ton force press into a pill with 13 mm diameter and 1 mm thickness. Samples having uniform thickness in the 0.7-1 mm range were placed between gold plated round electrodes, the upper electrode having a 20 mm diameter. The measurements for *electric breakdown strength (EBD)* were performed on a Trek installation with the following parts: high-speed high-voltage power amplifier, function generator, and oscilloscope. The electrodes (2.5 cm diameter) consisting of aluminum discs were applied on the film samples and a voltage increase rate of 500 $V \cdot s^{-1}$ was used for the measurements, with the environment conditions as such: room temperature (20 ºC) and relative humidity RH~70-72%. Before the measurements all the samples were maintained in the equipment room in order to reach equilibrium with the environmental humidity. For each sample, three tests were performed, with the smallest value taken into account.

2.3. Procedure

2.3.1. Preparation of composite materials and film formation

The crystalline complexes, CuC, NiC and CoC powdered by manually grinding were incorporated in well-determined amounts, according to Table 2, within the polysiloxane matrix. A double roll Yanke-Kunkel laboratory mixer with palettes in Dublex system was used to achieve a homogeneous mixture of the synthesized siloxane with various amounts of additions. Besides the metallic complex, 8 wt% silica and 2 wt% DCBP were also incorporated in each mixture. Reference samples were prepared without metal complexes in their composition: GC0 consisting of pure PDMS crosslinked with 2 wt% catalyst (DCBP) and GC1 in which, besides the catalyst, 8 wt% reinforcing filler (Aerosil) was added. For each composition, the formed mixture was put in an iron mold, which was pressed between two metal sheets in order to form elastomer films with a square surface of 100x100 mm and a thickness of up to 1 mm and then was kept in an oven at 180 ºC for two hours in order to achieve crosslinking by radicalic reaction, and was further kept at 160 ºC for three hours for ageing of the films (Scheme 2). Sample GC7 was kept at high temperature for a shorter time (1 hour) instead of the standard time (2 hours) for other samples (such as GC6) in order to test the influence of crosslinking time. The mold was extracted from the oven, and the film was peeled off of it.

3. Results and discussion

Three complexes of Cu(II), Ni(II) and Co(II) were prepared and characterized as reported in previous works.[31,32] These are tetra-, di- or mononuclear complexes of triethanolamine (Figure 1) formed in different conditions and are used as fillers for PDMS. The polar metal coordinated core units (blue moiety) and chlorine (green) should induce an increase in the dielectric

permittivity of the resulting material, while the ethylene bridges (grey moieties) that surround them can ensure compatibility with non-polar silicone matrix.

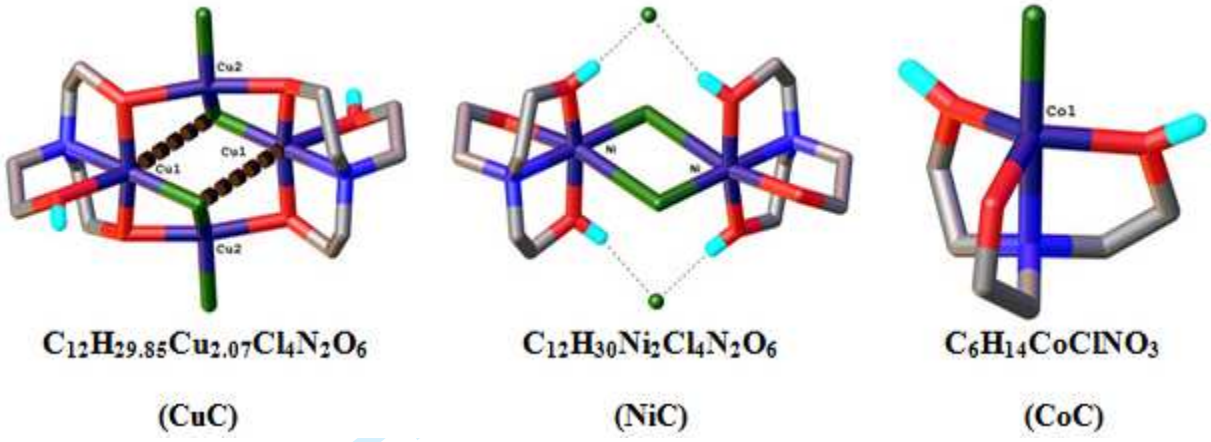

Figure 1. Structures of the metal complexes generally abbreviated as MC used as fillers [31,32].

Analysis by dielectric spectroscopy reveals, as was expected, very high values for dielectric permittivity but also for dielectric loss for these compounds falling rather in semiconductor domain (Figure 2, Table 1).

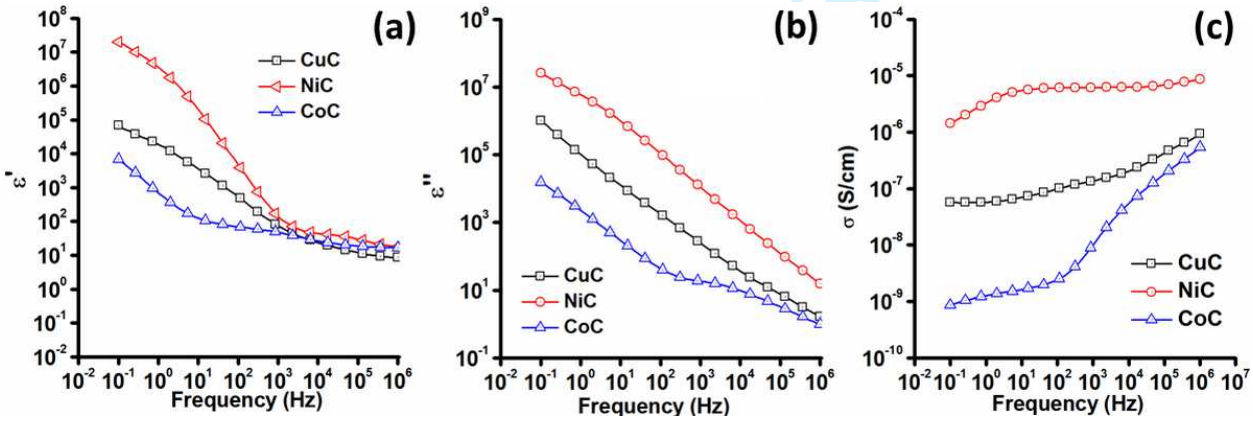

Figure 2. Dielectric spectra for the metal complexes CuC, NiC and CoC

Table 1. Main characteristics of the metal complexes determined on the basis of dielectric spectra

Sample	ε` (10 Hz)	ε`` (10 Hz)	σ(S/cm) (10 Hz)	ε` (10^5 Hz)	ε`` (10^5 Hz)	σ (S/cm) (10^5 Hz)
CuC	3380	11700	7.01×10^{-8}	8.51	1.67	9.31×10^{-7}
NiC	178000	928000	5.55×10^{-6}	17.8	15.7	8.71×10^{-6}
CoC	122	275	1.64×10^{-9}	16.7	0.975	5.42×10^{-7}

The nickel complex shows the highest values for dielectric permittivity but also for dielectric loss and conductivity (ε`=178000 and 17.8; ε``= 928000 and 15.7; σ = $5.55 \times 10^{-6}$ and $8.71 \times 10^{-6}$ S/cm S/cm at 10, and $10^5$ Hz, respectively), while in the case of the cobalt complex, they are somewhat lower (ε`=122 and 16.7; ε``= 275 and 0.975; σ = 1.64×10^{-9} and 5.42×10^{-7} S/cm). The dielectric parameters of the copper complex, especially at lower frequencies, are between the other two. Although in all cases there is a decrease of dielectric permittivity with increasing frequency, it still retains a higher value (ε' > 10) as compared with those specific for siloxanes (ε'~3) even at 10^6 Hz. This behavior determined our choice for using these complexes as fillers in the preparation of dielectric elastomers, as there is no mention in scientific literature for previous use of such complexes for this purpose. Therefore, all three crystalline complexes were finely ground and incorporated in PDMS in the amounts provided in Table 2 by applying the sequence of operations shown in Scheme ESI1. Silica in percentage of 8 wt% was also incorporated as reinforcing filler in order to ensure good mechanical characteristics. After incorporation by mechanical mixing and homogenization, the mixtures were processed as films and crosslinked by a radicalic mechanism initiated by DCBP under high pressure and at 180 ^{o}C.

Both polymer and the metal complexes are thermally stable up to 200 °C and even higher, as proved by thermogravimetrical analysis.[28] In these conditions, the peroxide decomposes generating highly active radicals that rip hydrogen atoms randomly from the organic groups attached to the silicon atoms along the siloxane chains or even from the metal complex molecules. The formed radicals quickly combine with each other leading to stable crosslinks. The residual peroxides and decomposition products were removed in the post curing period.

Table 2. Feed amounts of the components for composites preparation and sorption data (2 wt% catalyst, DCBP, was added in all mixtures; high temperature crosslinking time: 2 h)

Sample	SiO_2, wt%	MC	MC, wt%	Total water sorption, wt% (dry basis) at RH = 90%, T = 25 °C
GC0	0	-	0	0.98
GC1	8	-	0	1.04
GC2	8	CuC	2	1.25
GC3	8	CuC	8	2.70
GC4	8	NiC	2	1.15
GC5	8	NiC	8	1.81
GC6	8	CoC	2	0.91
GC7 [a]	8	CoC	2	1.82
GC8	8	CoC	8	2.90

[a] high temperature crosslinking time: 1 h.

On the SEM images taken in cryofractured section, particles/agglomerates of micrometer size are evenly distributed within the polymeric matrix (Figure 3). Elements mapping performed by EDX analysis (Figures ESI2 and ESI3) highlights a distribution of metal centers, which follows roughly the same pattern of nanoparticles seen through SEM.

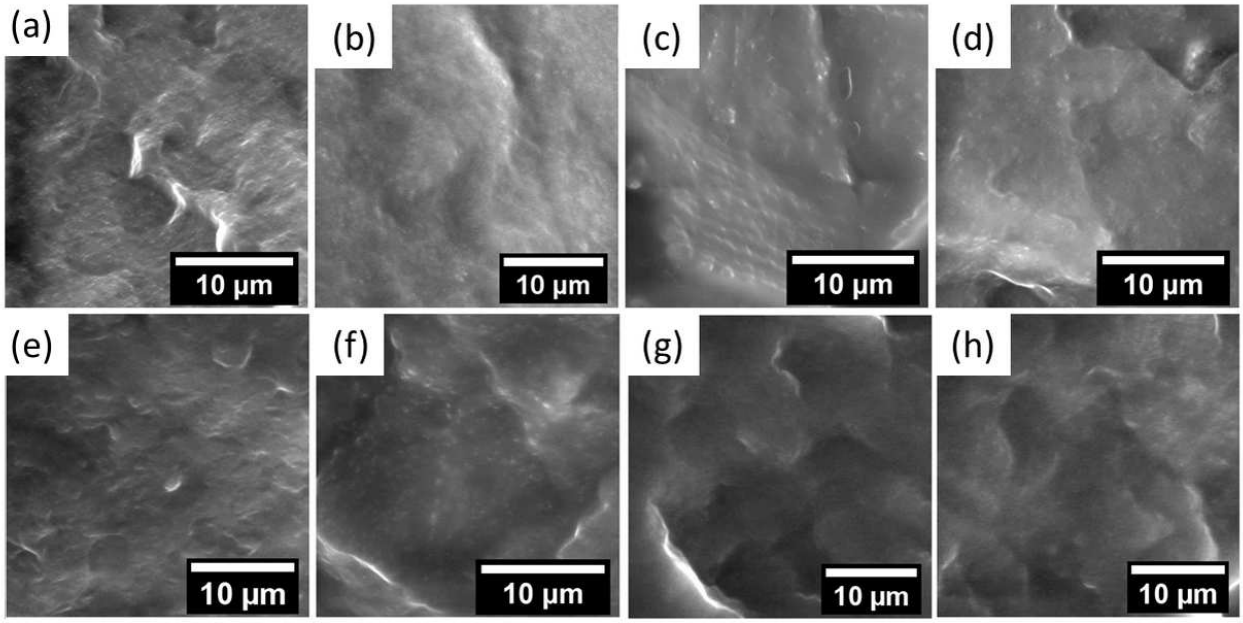

Figure 3. SEM images of the fractured composite films: a) GC1; b) GC2; c) GC3; d) GC4; e) GC5; f) GC6; g) GC7; h) GC8

The targeted application for dielectric elastomers (electromechanical devices) requires environmental stability over time, besides adequate mechanical and dielectric characteristics. For example, moisture sorption could affect the value of the dielectric permittivity and implicitly electromechanical behavior of materials. Therefore, the moisture sorption isotherms have been recorded at 25 ºC for all the samples prepared (Figure 4). The isotherms show similar variation in controlled-humidity atmosphere for the three different types of complexes but with different maximum sorption values (Table 2). The difference between the isotherms of reference sample

GC0 consisting in pure crosslinked siloxane polymer and reference sample GC1 containing treated silica is minimal, proving the good dispersion of silica nanoparticles in the siloxane matrix and the efficiency of hydrophobization treatment of the silica nanoparticles. For all three metal complexes used, the sorption capacity increases with increasing weight percentage of complex added in the formulation of the sample. Thus, the water sorption capacity of reference GC0 is the lowest value (0.98 wt%), while GC7, with 2 wt% cobalt complex content has 1.82 % weight change and GC8, with 8 wt% cobalt complex, has the highest sorption value, 2.90 wt% (Table 2). This behaviour is due to the polar nature of the metal complexes incorporated. The sharp increase of the moisture sorption at RH values over 40% suggests formation of a hydrate.[35] A molar ratio water:metal complex of 4:1 was estimated based on the amount of water taken by sorption in the material, similar to the one found for single metal complexes.[31] This behavior is more accentuated for samples containing copper and cobalt. At the end of the sorption–desorption cycle, the weight of the sample reverts in all cases to the initial point, showing the moisture stability of the samples at room temperature.

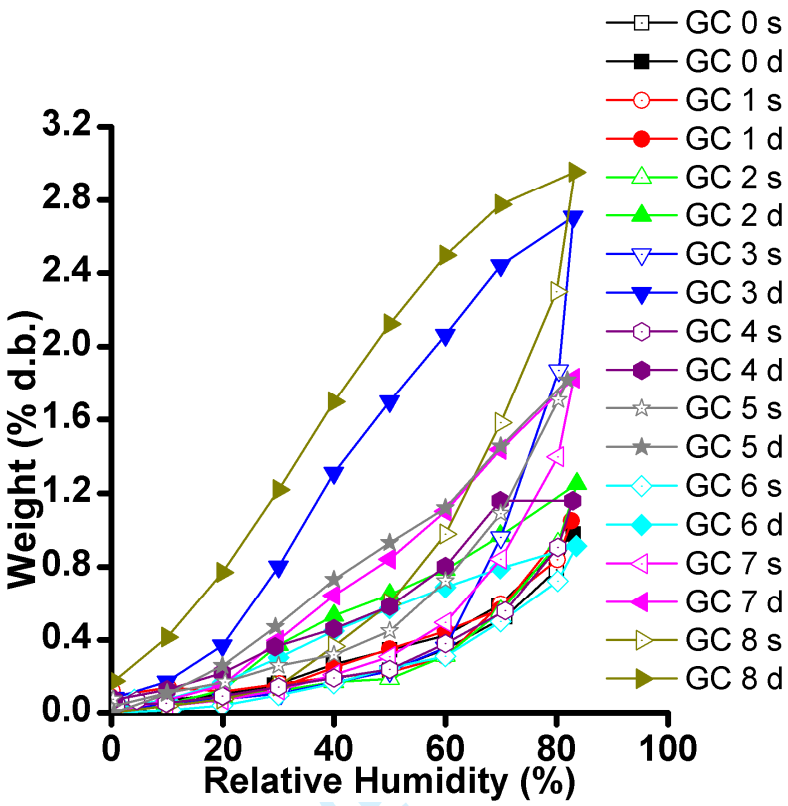

Figure 4. Sorption/desorption isotherms for the prepared samples (S, sorption; D, desorption)

Both dielectric and mechanical properties are influenced by the crosslinking degree of the samples. Although crosslinking has been made under the same conditions, except sample GC7, it would be expected the presence of different metal complexes influences in different ways the crosslinking kinetic and pattern. In order to evaluate the crosslinking yield, the swelling capacity of the hybrid networks was evaluated gravimetrically. Two solvents with different polarities (water and chloroform) were chosen. The swelling was performed by immersion of the weighed samples in high excess of solvent and maintained in static regime at room temperature for 48 h. After that, these were wiped easily with filter paper and weighed again. The solvent uptake capacity (W) is determined from the equation:[35]

$$W[g/g] = (W_w - W_d)/W_d \qquad (4)$$

where W_w and W_d are the weights of the swollen and the dry sample in equilibrium conditions. The equilibrium solvent uptake values at room temperature are presented in Table 2. Pure non-crosslinked polydimethylsiloxane (GC00) is soluble in chloroform. Swelling measurements data is used to estimate the crosslinking density in polymer networks.[36] The samples prepared have low sorption capacity values, both for water and for chloroform. Therefore classical equations of Flory-Rehner[37] or Peppas-Merrill[38,39] generally used for absorbent hydrogels could not be used for the samples due to the high degree of crosslinking and the hydrophobicity of siloxane. The crosslinking yields, C_y, and the weight losses, L_w, were calculated for the samples:

$$C_y = W_e / W_d \quad (5)$$

$$L_w = (W_d - W_e) / W_d \quad (6)$$

where W_d is the weight of the dried sample before swelling and extraction, W_e is the weight of the dried sample after extraction and ($W_d - W_e$) is the weight of the non-crosslinked fraction removed by extraction (Table 3). The results showed large crosslinking yields and limited weight losses for the samples.

The crosslinking density can also be estimated from the DSC data:

$$\rho_c = (C_p^i - C_p^0) / C_p^0 \quad (7)$$

where C^i_p and C^0_p are the heat capacities of the polymer network at a given crosslinking density and of the non-crosslinked polymer, respectively.[36,37] DSC curves were recorded in the range −150 ÷ +50 ºC. The data obtained from DSC analysis (Figure ESI4) show that all crosslinked samples have T_g values in the range -121 ÷ -125 ºC. This proves the metal complexes are well embedded in the siloxane network and do not significantly modify the T_g of siloxane at -124 ºC. The heat capacity value of this transition was taken into consideration to estimate crosslinking density (eq. 7) for some of the prepared samples. The obtained data for the crosslinking degree

has specific values for each type of metal complex sample, but it increases with the content of metal complex for every metal used (from 0.05 to 0.32, from 0.03 to 0.13 and from 0.19 to 0.23 for the samples containing CuC, NiC and CoC in percentages of 2 and 8 wt%, respectively) (Table 3). The same trend can be noticed in the values of the crosslinking yield estimated on the basis of swelling measurements. This shows the microparticles of metal complex act as centers for crosslinking in radical condensation.

Table 3. Data for crosslinking degree of silicone-metal complex composites measured from swelling in solvent and DSC measurements

Sample	Solvent uptake capacity ($g \cdot g^{-1}$)[a]		Crosslinking yield, C_y[b]	Weight loss, L_w[c]	Heat capacity, C_p ($J \cdot g^{-1} \cdot K^{-1}$)	Crosslinking density, ρ_c ($mol \cdot cm^{-3}$)[d]
	Water	Chloroform				
GC00[e]	0.010	dissolution	0	1	0.100	-
GC0	0.007	7.26	0.852	0.148	0.115	0.15
GC1	0.012	5.62	0.943	0.057	0.152	0.52
GC2	0.126	8.00	0.750	0.250	0.105	0.05
GC3	0.300	12.03	0.867	0.133	0.068	0.32
GC4	0.114	6.53	0.948	0.052	0.097	0.03
GC5	0.045	5.75	0.952	0.048	0.087	0.13
GC6	0.091	6.04	0.941	0.059	0.119	0.19
GC7	0.200	7.22	0.934	0.066	0.087	0.13
GC8	0.472	6.92	0.951	0.049	0.123	0.23

[a]Equation (4); [b]Equation (5); [c]Equation (6); [d]Equation (7); [e]raw PDMS.

DSC curves (Figure ESI4) highlight also one exothermic peak at about -68/-74 °C and an endothermic peak at -37/-42 °C), assigned to the phenomenon of cold crystallization and the melting or crystalline phase. The peak corresponding to melting (-38 °C) is similar to the one corresponding for crystallization (-70 °C) (with ΔH values of around -19 ÷ -23 J/g for crystallization and 19 ÷ 23 J/g for melting), and this indicates that a small amount of crystalline phase develops during the cooling scan due to the high degree of crosslinking. The variation of temperatures for crystallization and melting for the reference samples GC0 and GC1 in relation to pure siloxane polymer GC00 shows that the crosslinking induces changes in the behaviour of the siloxane (Figure ESI4a). The sample GC7 which was crosslinked at 180 °C for only one hour shows larger crystallization and melting peaks (ΔH = 21.5 J/g for melting, ΔH = -23 J/g for crystallization) than sample GC6 (ΔH = 19.1 J/g for melting, ΔH = -20.8 J/g for crystallization), as the smaller degree of crosslinking, and therefore, the higher freedom degree of the siloxane chains determines the formation of a larger amount of crystalline phase (Figure ESI4c). The same behaviour is seen for sample GC4, which has a smaller degree of crosslinking than sample GC5. The difference in the areas of the melting and crystallization peaks for the prepared samples show that both the crosslinking degree and the nature of the metal influence the thermal behavior of the elastomer samples, but the influence of the degree of crosslinking (also influenced by the percentage of metal complex in the sample) is more significant than the influence of the type of metal complex used.

The samples were subjected to stress-strain tests at room temperature. As expected, the sample GC1 containing 8 wt% silica nanoparticles shows a slight increase in the breaking stress value when compared with pure siloxane sample GC0 but a significant decrease in breaking strain, from 360 % of initial length (GC0) down to 240 % of initial sample length (GC1) (Figure 5,

Table 4). The samples with each type of metal complex (GC2 and GC3 for copper, GC4, GC5 for nickel and GC6, GC7 and GC8 for cobalt complex) show lower breaking stress values when compared with the reference samples and a clear decrease of these by increasing content of complexes from 2 to 8 wt%. The breaking strain value decreases even more as the content of metal complex increases in special in the case of those based on nickel. This behaviour is due to the low degree of compatibility of the polar metal complexes with nonpolar silicone matrix favoring formation of agglomerated particles with micrometer size that are not acting as reinforcing filler (the case of silica nanoparticles) but as stress concentrator, leading to early rupture of the sample where microscopic defects are in the elastomer sample. The samples with copper-based complexes have also smaller breaking stress values but show improved breaking strain, in comparison with reference samples GC0 and GC1, this increasing with the content of complex in the sample up to 580 % for 8 % Cu complex content (Figure 5, Table 4). This could be because in complex structure (Figure 1), the polar part is better enveloped by nonpolar alkyl moieties confering improved compatibility with the siloxane matrix.

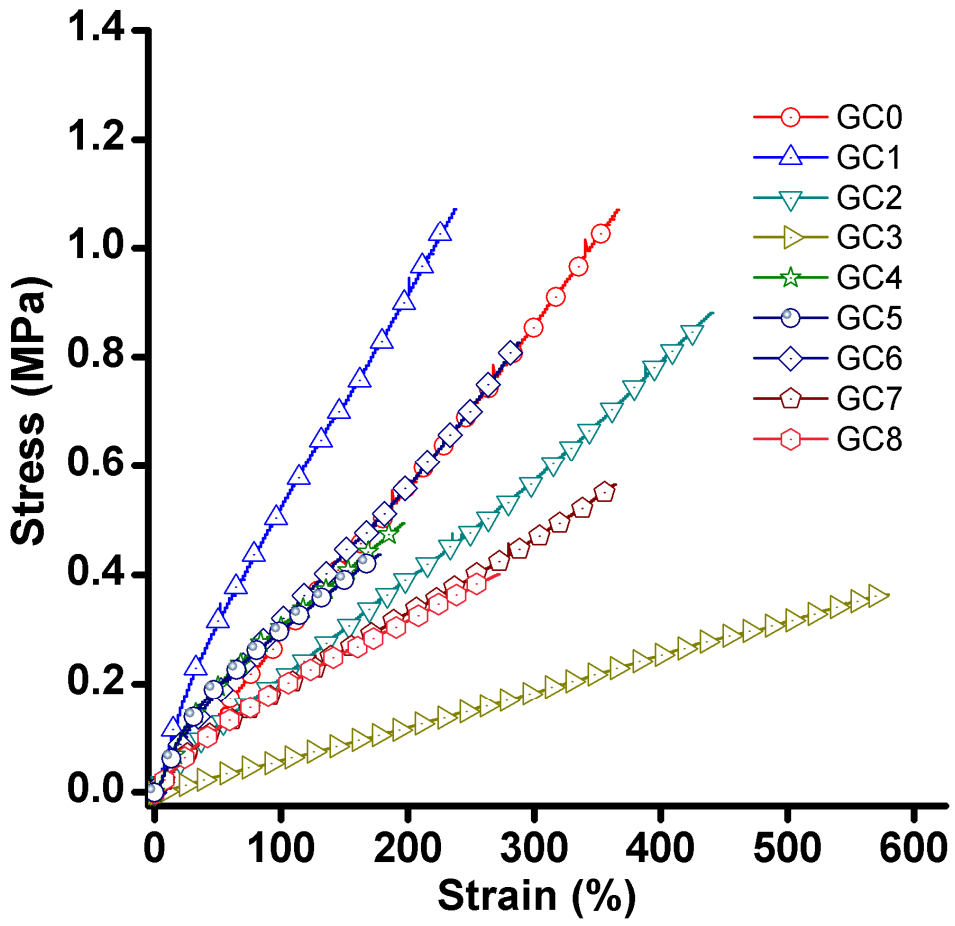

Figure 5. Stress–strain curves for crosslinked samples

The Young modulus at maximum strain for each sample shows that the samples containing metal complexes have smaller values of this parameter than the reference sample with silica (GC1) and even less than pure crosslinked siloxane (GC0) (Figure 6). This leads to the conclusion that the metal complex particles, especially copper and nickel derivatives, act as a bulk softening filler, thus nullifying the mechanical reinforcing effect of silica and explaining the larger values recorded for the breaking strain. In the case of cobalt complex, this effect is diminished, the behaviour of the samples being closer to that of pure crosslinked silicone.

Table 4. The main results of tensile tests and dielectric measurements for the prepared composites

Sample	E[a], MPa	σ[b], MPa	ε[c], %	ε` (10 Hz)	ε``x10^3 (10 Hz)	ε` (10^5 Hz)	ε``x10^3 (10^5 Hz)	β[d] (MPa^{-1})	Utt[e], KJ/m^3
GC0	0.221	1.048	360	3.43	5.50	3.42	0.14	15.52	18.38
GC1	0.768	1.080	240	3.50	4.78	3.52	0.08	4.56	14.10
GC2	0.277	0.846	423	3.51	5.73	3.53	0.22	12.67	17.67
GC3	0.023	0.364	580	3.58	15.50	3.54	0.20	155.65	7.43
GC4	0.524	0.494	197	3.61	22.00	3.55	0.23	6.89	5.72
GC5	0.521	0.437	178	3.87	82.70	3.53	8.25	7.43	4.67
GC6	0.275	0.826	288	3.59	17.40	3.55	0.12	13.05	7.85
GC7	0.465	0.565	364	3.48	18.50	3.46	0.08	7.48	12.19
GC8	0.289	0.401	272	3.82	43.40	3.60	7.80	13.22	6.26

[a]Young's modulus (calculated at 10% strain); [b]stress at break; [c]elongation at break; [d]electromechanical sensitivity calculated according to ref.[25]; [e]Ultimate tensile toughness.

The value of the area integrated under the entire stress-strain curve, known as ultimate tensile toughness (Utt), was estimated, being considered as a measure of the amount of energy per volume that a material can absorb to break.[40–42] This is an indication on the suitability of such materials for energy harvesting application. Excepting the sample GC2 that shows a higher value for Utt (17.67 KJ/m^3), the other samples are below those of the reference sample GC1 (Table 4).

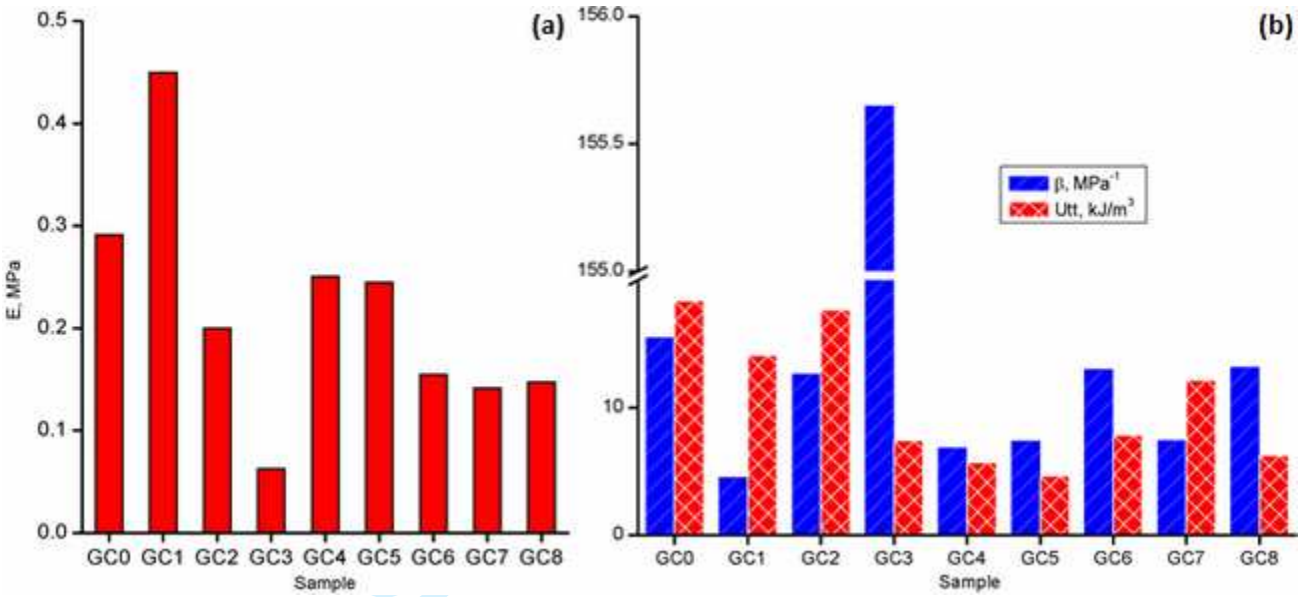

Figure 6. Comparative values for Young's modulus (calculated at maximum strain) – (a); electromechanical sensitivity, β, calculated according to ref.[25] and ultimate tensile toughness (Utt) – (b) for the prepared composites.

Although the dielectric permittivity values of the complexes themselves are large, there were only slight increases in the dielectric permittivity of the silicone as a result of the incorporation of the metal complexes, in the range 3.48-3.87 as compared with 3.43 for GC0 reference sample (Figure 7a, Table 4). A chemical modification/degradation of the complexes during the radicalic crosslinking process after which the polar character of the complex diminishes could be an explanation for this.

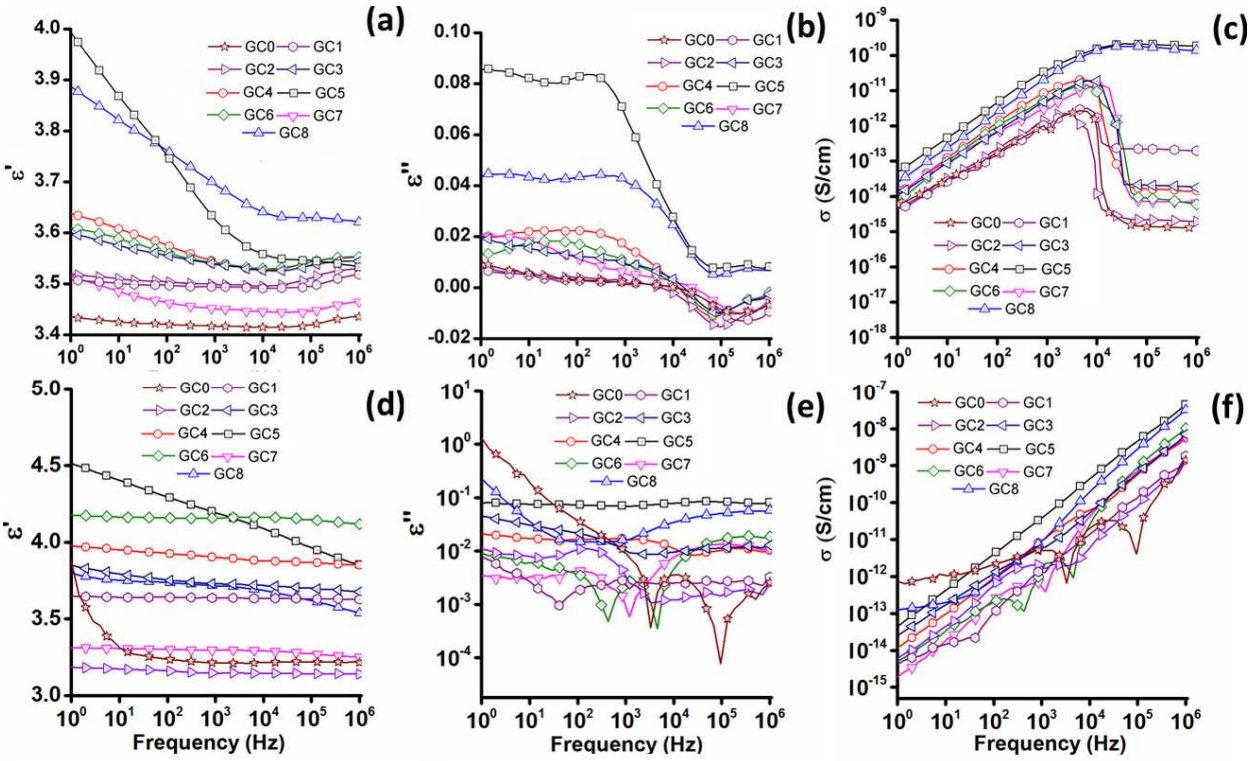

Figure 7. Dielectric spectra for cross-linked pristine films - a,b,c, and after mechanical cycles - d,e,f

When comparing samples GC6 and GC7, both having the same content and type of metallic complex, the sample GC7 with a crosslinking degree lower, due to the conditions in which it was made, has a smaller value for the real part of the dielectric constant. This value is lower even than that of the sample GC1 containing only silica nanoparticles, thus demonstrating the importance of a good treatment for crosslinking in order to bind the particles of filler. The largest values for the dielectric permittivity at low frequency (10 Hz) of 3.82 and 3.87, important for energy harvesting and low frequency actuation, were recorded for samples GC5 and GC8 containing 8 wt% NiC and CoC complexes, respectively. However, this reflects in higher electromechanical sensitivity β, calculated as the ratio between the dielectric permittivity value at 10 Hz and elastic modulus,[25] only in the case of the sample GC8 (13.22 MPa^{-1}), while in the case

of GC5 this is low enough (7.43 MPa^{-1}) mainly due to the high value of the elastic modulus (0.521 MPa). The highest value, 155.65 MPa^{-1}, was obtained for the sample GC3 that shows the lowest Young`s modulus (0.023 MPa) (Table 4). Loss factor, although it is slightly higher in metal complexes composites than in reference samples GC0 and GC1, it is maintained at low values ($<10^0$) specific for electrically non-conducting materials (Figure 7b). At around 10^4 Hz frequency, a drop in both dielectric permittivity and loss is observed (Figure 7a,b). Lowering the latter being more pronounced (the largest decrease, of 0.08 units, was recorded in the case GC5 sample) makes the loss tangent (tan $\delta = \varepsilon'/\varepsilon''$) does not increase, but it decreases, which is desirable. The conductivity values (Figure 7c) show the samples are dielectric in the range of frequencies studied (1-10^6 Hz), preserving the electrical non-conducting character of siloxane.

Cyclic mechanical stresses consisting in 50 repeated equiaxial deformations up to 50% compared to the initial diameter were performed in order to estimate the changes occurred in the dielectric characteristics. Slight increases in both the value of the dielectric permittivity and the losses, as well as a flattening of the curves throughout the frequency range are observed (Figure 7d,e, Table 5). These changes are due to rearrangement of filler nanoparticles within the polymer matrix, along with the decreasing in free volume after the Mullins effect disappearance. This effect is observed in conductivity spectrum, when at high frequency the samples almost overcome the insulator domain, being close to semiconductor domains (~10^{-8} S/cm, Figure 7f).

Table 5. The main results of the dielectric measurements for the prepared composites after cyclical mechanical stretch

Sample	ε` (10 Hz)	ε``x10^3 (10 Hz)	ε` (10^5 Hz)	ε``x10^3 (10^5Hz)	σ (S/cm) (10 Hz)
GC0	3.30	175.4	3.21	3.56	$1.05x10^{-12}$
GC1	3.64	2.53	3.63	2.47	$1.51x10^{-14}$
GC2	3.17	7.81	3.15	1.21	$4.67x10^{-14}$
GC3	3.79	30.17	3.72	9.42	$1.8x10^{-13}$
GC4	3.94	17.16	3.87	11.65	$1.02x10^{-13}$
GC5	4.4	74.89	4.10	78.19	$4.47x10^{-13}$
GC6	4.16	6.03	4.16	3.99	$3.61x10^{-14}$
GC7	3.30	3.31	3.29	7.2	$1.97x10^{-14}$
GC8	3.75	34.12	3.68	33.62	$2.04x10^{-13}$

To measure the dielectric strength of the films that originally had 0.7-1.0 mm thick, too high to be pierced with a maximum voltage applied of 20 kV (the maximum capability of our setup), these were equiaxially stretched to be thinned to lower thicknesses (200-300 μm) using a home-made device. Only then it could be recorded the electric breakdown values (EBD, MV/m) (Figure 8). As expected, the introduction of metal complexes particles leads to decreases of EBD (from 67 MV/m for GC0 to 23 MV/m for GC8), because the metal complex particles that are close to each other can form pathways for transmission of the current.

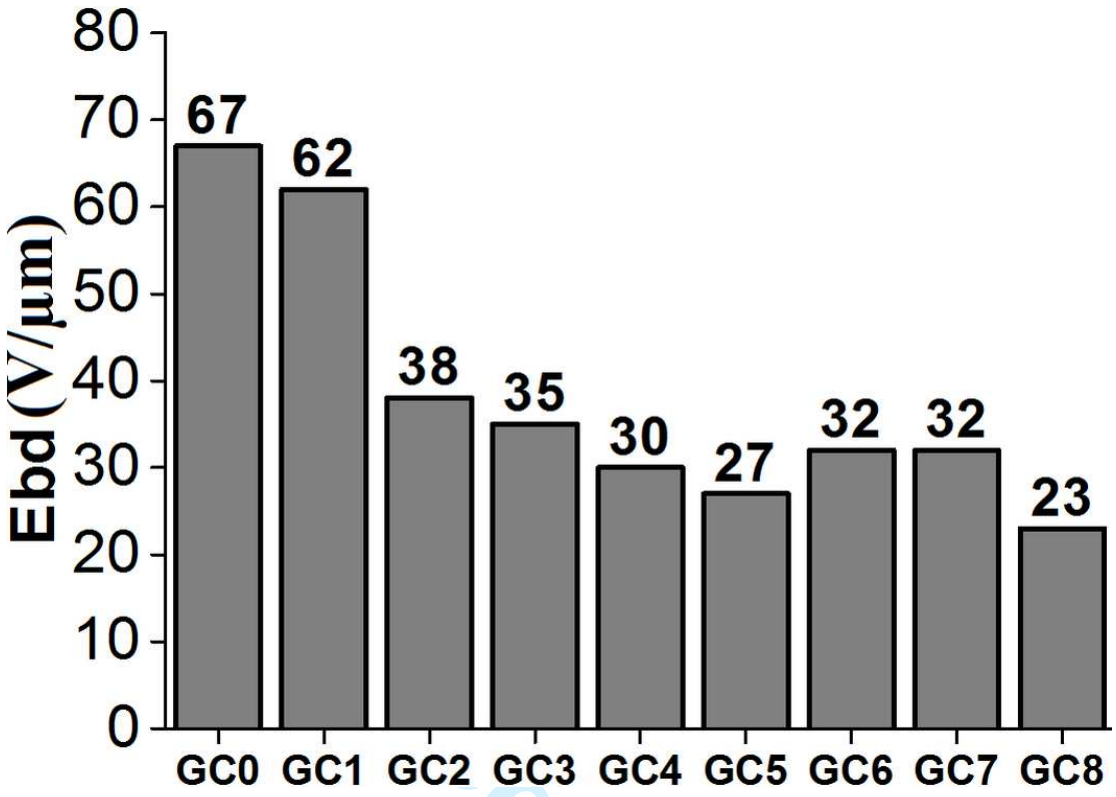

Figure 8. Electric breakdown values for the samples (V/µm)

4. Conclusions

New dielectric elastomers were prepared as composite materials by incorporating transition metal complexes, besides silica, as active fillers for a polydimethylsiloxane matrix. A simple, affordable method consisting in mechanical mixing of components and radical crosslinking was used. Thermal transitions occur around the same temperature values for all prepared samples, the differences consisting in heat capacity of these correlated with crosslinking degree, which in turn is influenced by the nature of the metal complex and curing duration. The presence of the fillers, metal complexes especially due to their polar nature, induces a slight increasing in moisture sorption of the silicone up to 2.90 % in the case of sample containing 8 wt% cobalt complex, towards 0.98 wt% for pure crosslinked silicone. The samples containing copper complex show

increased breaking strain values in comparison with the pure or silica-filled silicones (GC0 and GC1). The incorporation of these complexes having very high dielectric permittivity values in silicone matrix resulted in an increase in the value of this feature of the latter with up to 33 % (composite with 8 wt% nickel complex) while the loss factor (ε") increases, but it is maintained at low values ($<10^0$) specific for electrically non-conducting materials. Slightly increased values of these characteristics were recorded after repeated equiaxial deformations of the films.

The conductivity values for the samples are low ($\sigma<10^{-9}$ S/cm), specific for dielectric materials. The overall properties of the dielectric elastomers with metal complexes show these membranes and especially the ones with copper complex, are suitable for use as dielectric elastomers. The overall properties but in particular parameters of interest for electromechanical applications indicate the composites incorporating copper complex as most suitable for electromechanical application having better values either for ultimate tensile toughness (17.67 KJ/m^3 for sample GC2 with 2 wt% copper complex) or electromechanical sensitivity (155.65 MPa^{-1} for sample GC3 with 8 wt% copper complex) than the reference sample containing only silica (GC1) and the highest EBD values (38 and 35 V/μm for GC2 and GC3 samples, respectively) among the metal complex-containing composites.

Acknowledgements: The work presented in this paper is developed in the context of the project PolyWEC (www.polywec.org, prj. ref. 309139), a FET-Energy project that is partially funded by the 7th Framework Programme of European Community and co-financed by Romanian National Authority for Scientific Research, CNCS-UEFISCDI (Contract 205EU). The authors address many thanks to Dr. Stelian Vlad for mechanical measurements

References

1. Bar-Cohen, Y. *Electroactive Polymer (EAP) Actuators as Artificial Muscles: Reality, Potential, and Challenges*. (SPIE Press, 2001).

2. Pelrine, R. High-Speed Electrically Actuated Elastomers with Strain Greater Than 100%. *Science (80-.).* **287,** 836–839 (2000).

3. Matysek, M., Lotz, P. & Schlaak, H. F. Braille display with dielectric polymer actuator. in *Proceedings 10th Int. Conf. New Actuators* 997–1000 (2006).

4. Flittner, K., Schlosser, M. & Schlaak, H. F. Dielectric elastomer stack actuators for integrated gas valves. in *SPIE Smart Structures and Materials + Nondestructive Evaluation and Health Monitoring* (eds. Bar-Cohen, Y. & Carpi, F.) 79761K–79761K–7 (International Society for Optics and Photonics, 2011). doi:10.1117/12.880050

5. Kornbluh, R. D., Pelrine, R., Prahlad, H. & Heydt, R. Electroactive polymers: an emerging technology for MEMS. in *Micromachining and Microfabrication* (eds. Janson, S. W. & Henning, A. K.) 13–27 (International Society for Optics and Photonics, 2004). doi:10.1117/12.538382

6. McKay, T., O'Brien, B., Calius, E. & Anderson, I. An integrated, self-priming dielectric elastomer generator. *Appl. Phys. Lett.* **97,** 062911 (2010).

7. Carpi, F., Frediani, G., Turco, S. & De Rossi, D. Bioinspired Tunable Lens with Muscle-Like Electroactive Elastomers. *Adv. Funct. Mater.* **21,** 4152–4158 (2011).

8. Zhao, X., Hong, W. & Suo, Z. Electromechanical hysteresis and coexistent states in dielectric elastomers. *Phys. Rev. B* **76,** 134113 (2007).

9. Carpi, F., Bauer, S. & De Rossi, D. Stretching dielectric elastomer performance. *Science* **330,** 1759–61 (2010).

10. Tuncer, E. & Sauers, I. in *Dielectric Polymer Nanocomposites* (ed. Keith, N. J.) 321 (Springer, 2009).

11. Koulouridis, S., Kiziltas, G., Zhou, Y., Hansford, D. J. & Volakis, J. L. Polymer–Ceramic Composites for Microwave Applications: Fabrication and Performance Assessment. *IEEE Trans. Microw. Theory Tech.* **54,** 4202–4208 (2006).

12. Opris, D. M. *et al.* New silicone composites for dielectric elastomer actuator applications in competition with acrylic foil. *Adv. Funct. Mater.* **21,** 3531–3539 (2011).

13. Vertechy, R., Fontana, M., Stiubianu, G. & Cazacu, M. Open-access dielectric elastomer material database. *Proc. SPIE* **9056,** 90561R–1–13 (2014).

14. Molberg, M. *et al.* Frequency dependent dielectric and mechanical behavior of elastomers for actuator applications. *J. Appl. Phys.* **106,** 054112 (2009).

15. Iacob, M. *et al.* Goethite nanorods as a cheap and effective filler for siloxane nanocomposite elastomers. *RSC Adv.* **5,** 45439–45445 (2015).

16. Momen, G. & Farzaneh, M. Survey of micro/nano filler use to improve silicone rubber for outdoor insulators. *Rev. Adv. Mater. Sci.* **27,** 1–13 (2011).

17. Khastgir, D. & Adachi, K. Rheological and dielectric studies of aggregation of barium titanate particles suspended in polydimethylsiloxane. *Polymer (Guildf).* **41,** 6403–6413 (2000).

18. Carpi, F., Gallone, G., Galantini, F. & De Rossi, D. in *Dielectric Elastomers as Electromechanical Transducers: Fundamentals, Materials, Devices, Models and Applications of an emerging electroactive Polymer Technology* (eds. Carpi, F., De Rossi, D., Kornbluh, R., Pelrine, R. & Sommer-Larsen, P.) 60 (Elsevier Ltd., 2008).

19. Gallone, G., Carpi, F., De Rossi, D., Levita, G. & Marchetti, A. Dielectric constant enhancement in a silicone elastomer filled with lead magnesium niobate-lead titanate. *Mater. Sci. Eng. C* **27,** 110–116 (2007).

20. Babar, A. A. *et al.* Performance of High-Permittivity Ceramic-Polymer Composite as a Substrate for UHF RFID Tag Antennas. *Int. J. Antennas Propag.* **2012,** ID 905409 (2012).

21. Nelson, J. K., Linhardt, R. J., Schadler, L. S. & Hillborg, H. Effect of high aspect ratio filler on dielectric properties of polymer composites: a study on barium titanate fibers and graphene platelets. *IEEE Trans. Dielectr. Electr. Insul.* **19,** 960–967 (2012).

22. Yansheng, Y. X. C. in *Multifunctional Polymer Nanocomposites* (eds. Jinsong, L. & Alan, K. T. L.) 466 (CRC Press, Taylor and Francis Group, 2011).

23. Sebastian, M. T. & Jantunen, H. Polymer-Ceramic Composites of 0-3 Connectivity for Circuits in Electronics: A Review. *Int. J. Appl. Ceram. Technol.* (2010). doi:10.1111/j.1744-7402.2009.02482.x

24. Huang, C. & Zhang, Q.-M. Fully Functionalized High-Dielectric-Constant Nanophase Polymers with High Electromechanical Response. *Adv. Mater.* **17,** 1153–1158 (2005).

25. Zhao, H., Wang, D.-R., Zha, J.-W., Zhao, J. & Dang, Z.-M. Increased electroaction through a molecular flexibility tuning process in TiO2–polydimethylsilicone nanocomposites. *J. Mater. Chem. A* **1,** 3140 (2013).

26. Shankar, R., Ghosh, T. K. & Spontak, R. J. Electroactive Nanostructured Polymers as Tunable Actuators. *Adv. Mater.* **19,** 2218–2223 (2007).

27. Zhou, Y. *et al.* The influence of pre-stressing on breakdown characteristics in liquid silicone rubber. *J. Electrostat.* **67,** 422–425 (2009).

28. Nguyen, H. C. *et al.* The effects of additives on the actuating performances of a dielectric elastomer actuator. *Smart Mater. Struct.* **18,** 015006 (2009).

29. Kofod, G. *et al.* Broad-spectrum enhancement of polymer composite dielectric constant at ultralow volume fractions of silica-supported copper nanoparticles. *ACS Nano* **5,** 1623–9 (2011).

30. Hu, W., Zhang, S. N., Niu, X., Liu, C. & Pei, Q. Aluminum nanoparticle/acrylate copolymer nanocomposites for dielectric elastomers with high dielectric constants. in *SPIE Smart Structures and Materials + Nondestructive Evaluation and Health Monitoring* (ed. Bar-Cohen, Y.) 90561O (International Society for Optics and Photonics, 2014). doi:10.1117/12.2045049

31. Dumitriu, A.-M.-C., Cazacu, M., Bargan, A., Shova, S. & Turta, C. Cu(II) and Ni(II) complexes with a tri-, tetra- or hexadentate triethanolamine ligand: Structural characterization and properties. *Polyhedron* **50,** 255–263 (2013).

32. Dumitriu, A.-C., Cazacu, M., Shova, S., Turta, C. & Simionescu, B. C. Synthesis and structural characterization of 1-(3-aminopropyl)silatrane and some new derivatives. *Polyhedron* **33,** 119–126 (2012).

33. Cazacu, M., Racles, C., Vlad, A., Antohe, M. & Forna, N. Silicone-based Composite for Relining of Removable Dental Prosthesis. *J. Compos. Mater.* **43,** 2045–2055 (2009).

34. Marcu, M., Simionescu, M., Cazacu, M., Lazarescu, S. & Ibanescu, C. Obtaining poly(dimethylsiloxane)α,ω-diols using the heterogeneous catalysis. The optimization of the reaction conditions. *Iran. J. Polym. Sci* **3,** 95–104 (1994).

35. Robert, L. H. & Hesse, N. D. Investigation of Pharmaceutical Stability Using Dynamic Vapor Sorption Analysis. *TA* TA337 (2007).

36. Vera-Graziano, R., Hernandez-Sanchez, F. & Cauich-Rodriguez, J. V. Study of crosslinking density in polydimethylsiloxane networks by DSC. *J. Appl. Polym. Sci.* **55,** 1317–1327 (1995).

37. Flory, P. J. & Rehner, J. Statistical Mechanics of Cross-Linked Polymer Networks II. Swelling. *J. Chem. Phys.* **11,** 521 (1943).

38. Peppas, N. A. & Merrill, E. W. Poly(vinyl alcohol) hydrogels: Reinforcement of radiation-crosslinked networks by crystallization. *J. Polym. Sci. Polym. Chem. Ed.* **14,** 441–457 (1976).

39. Peppas, N. A. & Merrill, E. W. Determination of interaction parameter χ1, for poly(vinyl alcohol) and water in gels crosslinked from solutions. *J. Polym. Sci. Polym. Chem. Ed.* **14,** 459–464 (1976).

40. Cole, M. A. & Bowman, C. N. Synthesis and Characterization of Thiol-Ene Functionalized Siloxanes and Evaluation of their Crosslinked Network Properties. *J. Polym. Sci. A. Polym. Chem.* **50,** 4325–4333 (2012).

41. Park, C. P. Toughened Blends of Polystyrene and Ethylene-Styrene Interpolymers. *J. Polym. Eng.* **21,** (2001).

42. Donald R. Askeland and Wendelin J. Wright. *The Science and Engineering of Materials, 7th Edition*. (2014).

Supporting Information

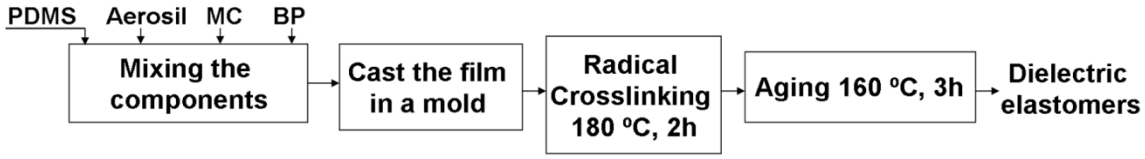

Scheme ESI1. Steps for the preparation process of composites with metal complexes

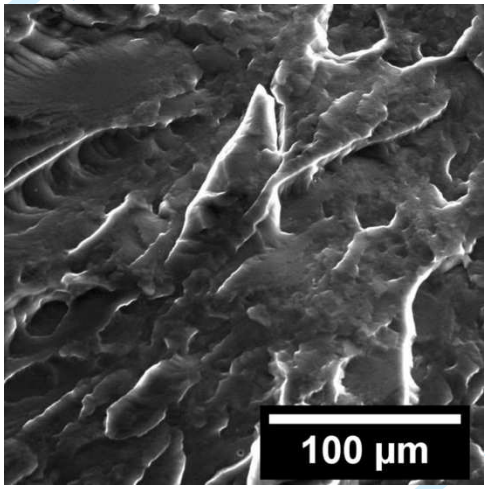

Figure ESI1. SEM image of cryofractured section of reference silicone film GC0

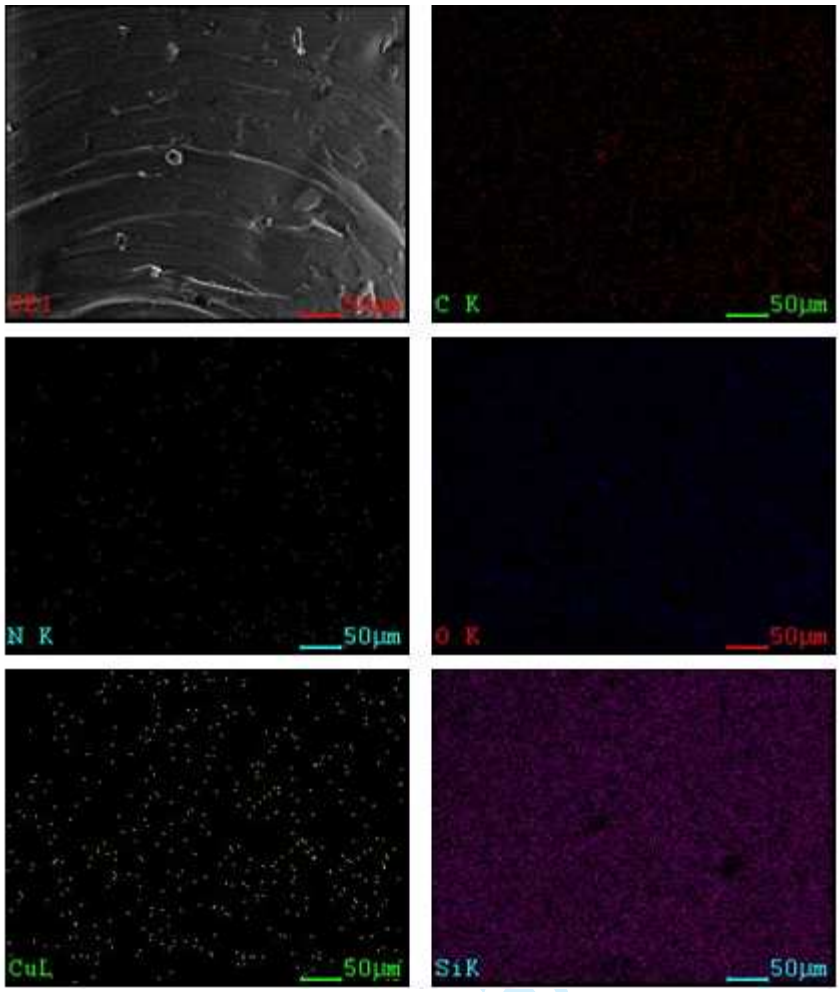

Figure ESI2. Elements mapping on the crosssection surface of film GC3

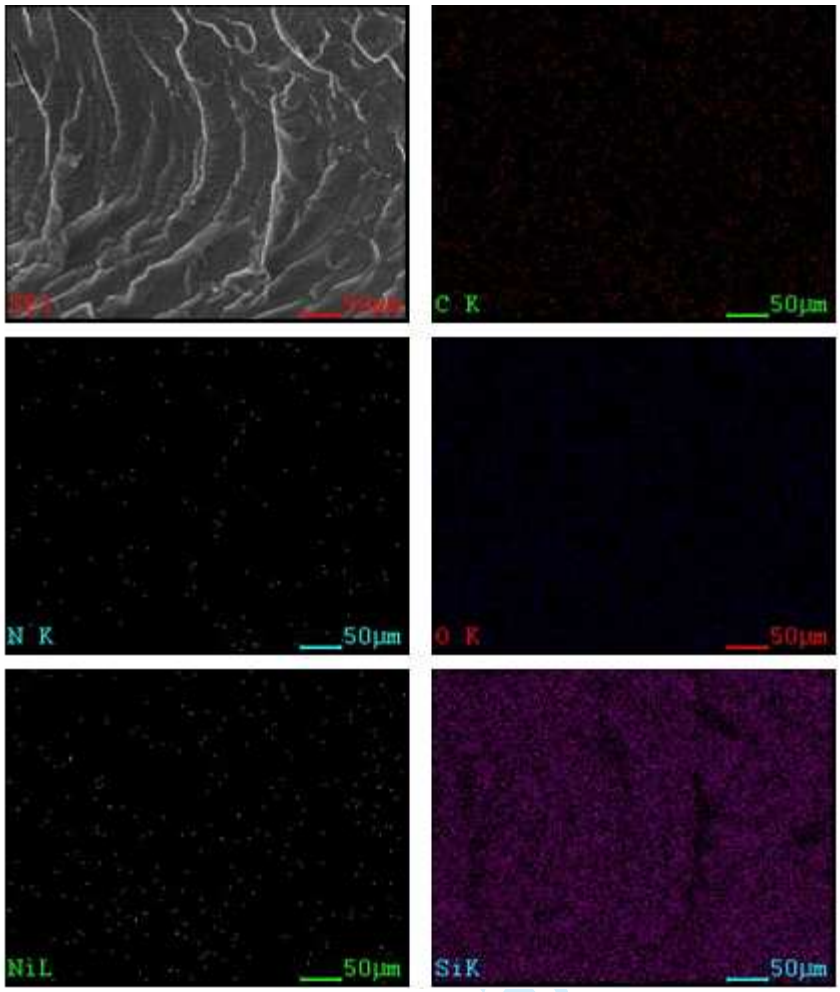

Figure ESI3. Elements mapping on the crosssection surface of film GC5

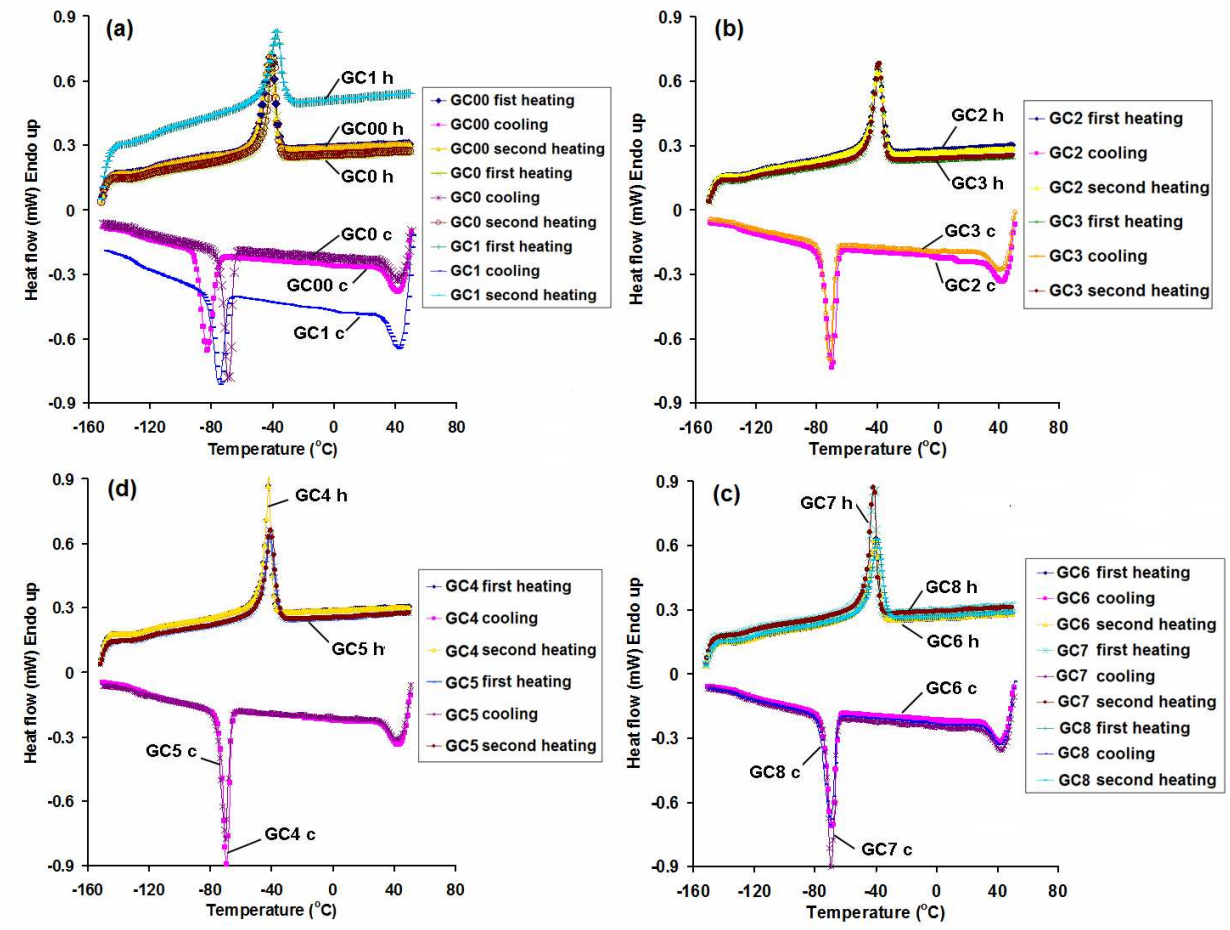

Figure ESI4. DSC results for the tested samples: (a) reference samples GC00, GC0, GC1; (b) samples with copper complex GC2, GC3; (c) samples with nickel complex GC4, GC5; (d) samples with cobalt complex GC6, GC7, GC8.